Received: 11 July 2023 | Revised: 5 February 2024 | Accepted: 26 March 2024

DOI: 10.1111/adb.13395

ORIGINAL ARTICLE

Addiction Biology SSA WILEY

The risk of cannabis use disorder is mediated by altered brain connectivity: A chronnectome study

Giovanni Fazio[1] | Daniele Olivo[1] | Nadine D. Wolf[2] | Dusan Hirjak[3] | Mike M. Schmitgen[2] | Florian Werler[2] | Miriam Witteman[4] | Katharina M. Kubera[2] | Vince D. Calhoun[5] | Wolfgang Reith[6] | Robert Christian Wolf[2] | Fabio Sambataro[1]

[1]Department of Neuroscience, Padua Neuroscience Center, University of Padua, Padua, Italy

[2]Department of General Psychiatry at the Center for Psychosocial Medicine, Heidelberg University, Heidelberg, Germany

[3]Department of Psychiatry and Psychotherapy, Central Institute of Mental Health, Medical Faculty Mannheim, Heidelberg University, Mannheim, Germany

[4]Department of Psychiatry and Psychotherapy, Saarland University, Saarbrücken, Germany

[5]Tri-institutional Center for Translational Research in Neuroimaging and Data Science (TReNDS), Georgia State University, Georgia Institute of Technology, Emory University, Atlanta, Georgia, USA

[6]Department of Neuroradiology, Saarland University, Saarbrücken, Germany

Correspondence
Fabio Sambataro, Department of Neuroscience, Padua Neuroscience Center, University of Padua, Via Giustiniani 5, Padova, Padua, Italy.
Email: fabio.sambataro@unipd.it

Funding information
This research did not receive any specific grant from funding agencies in the public, commercial or not-for-profit sectors.

Abstract

The brain mechanisms underlying the risk of cannabis use disorder (CUD) are poorly understood. Several studies have reported changes in functional connectivity (FC) in CUD, although none have focused on the study of time-varying patterns of FC. To fill this important gap of knowledge, 39 individuals at risk for CUD and 55 controls, stratified by their score on a self-screening questionnaire for cannabis-related problems (CUDIT-R), underwent resting-state functional magnetic resonance imaging. Dynamic functional connectivity (dFNC) was estimated using independent component analysis, sliding-time window correlations, cluster states and meta-state indices of global dynamics and were compared among groups. At-risk individuals stayed longer in a cluster state with higher within and reduced between network dFNC for the subcortical, sensory-motor, visual, cognitive-control and default-mode networks, relative to controls. More globally, at-risk individuals had a greater number of meta-states and transitions between them and a longer state span and total distance between meta-states in the state space. Our findings suggest that the risk of CUD is associated with an increased dynamic fluidity and dynamic range of FC. This may result in altered stability and engagement of the brain networks, which can ultimately translate into altered cortical and subcortical function conveying CUD risk. Identifying these changes in brain function can pave the way for early pharmacological and neurostimulation treatment of CUD, as much as they could facilitate the stratification of high-risk individuals.

KEYWORDS
cannabis, chronnectome, dynamic connectivity, magnetic resonance imaging, meta-states, resting state

Robert Christian Wolf and Fabio Sambataro contributed equally.

1 | INTRODUCTION

Cannabis is the third most widely used controlled substance in the world, after alcohol and tobacco, with estimates from the United Nations dating back to 2020, which indicate that 209 million people have used cannabis at least once in the previous year.[1] Among 1 in 10 regular users and 1 in 3 individuals using this substance daily[2,3] develop a problematic use with an inability to stop using cannabis despite clinical and psychosocial problems, that is, Cannabis Use Disorder (CUD).[4]

CUD has been associated with an increased risk of developing concomitant psychiatric disorders and contributes to the evolution of psychotic disorders in ultra-high risk subjects.[5] In this regard, observational and experimental studies have confirmed the association between cannabis consume and the onset and persistence of psychotic disorders with an effect size that is related to the duration of abuse and to the potency of cannabis.[6] In particular, cannabis use was linked with an earlier onset of psychosis, greater symptom severity, higher rates of relapse, longer hospitalizations and poorer outcomes.[7] Furthermore, chronic use of cannabis was also associated with a worse prognosis, including treatment resistance for various psychiatric disorders[8] and a greater risk of manic episodes and suicide.[6]

Several factors can contribute to the development of CUD in at-risk individuals. These include genetic and psychological factors (e.g., emotional dysregulation), comorbid mental disorders (including depression, anxiety, attention deficit hyperactivity disorder [ADHD], conduct and/or personality disorders), pattern of cannabis use (frequency and duration of use, concomitant use of alcohol and tobacco and other substances), parental cannabis use and stressful life events (childhood abuse, unemployment, financial difficulties).[9]

At the biological level, Koob and Volkow[10] propose a more general model of substance addiction that can be applied to cannabis addiction[11] and encompasses three stages: binge/intoxication, withdrawal/negative affect and preoccupation/anticipation. The first entails excessive impulsive and compulsive behaviours aimed at consuming cannabis despite the negative consequences associated with its use. This stage is characterized by hyperactivation of the mesocorticolimbic dopaminergic reward pathway caused by an impairment in incentive salience, which appears to drive dopaminergic signalling to maintain the drug consume upon exposure to conditioned cues and during tolerance development. These continuous mechanisms of opponent-process responses trigger the withdrawal/negative affect stage. This stage is characterized by neurobiological changes that take place within-systems, including decreased dopaminergic signalling in the nucleus accumbens (NAcc) and dorsal striatum that result in an elevation of reward thresholds for non-drug reinforcers, and between-systems, which include changes in the stress responses of the brain, including corticotropin-releasing factor (CRF) release in the amygdala and HPA-axis dysfunction. These changes can lead to loss of motivation for non-drug rewards and impaired emotion regulation during acute and sustained abstinence. The last stage, preoccupation/anticipation, is involved in the re-establishment of substance use after abstinence. At the neural level, the GABAergic and glutamatergic signalling pathways between the pre-frontal cortex (PFC) and the brain areas mediating decision-making, self-regulation, inhibitory control and working memory are altered. At the behavioural level, this stage may be associated with excessive salience attribution to drug-paired cues, decreases in responsiveness to non-drug cues and reinforcers and reduction of the ability to inhibit maladaptive behaviour.[10,11] Overall, the neural changes implicated in vulnerability and the risk of developing CUD need to be further explored.

Neuroimaging studies have shown that the brain is intrinsically organized in functionally connected networks that interact with each other to determine a specific function and their spontaneous activity can be studied using resting state functional Magnetic Resonance Imaging (rs-fMRI) rather than using specific tasks that engage few regions and can be influenced by performance.[12] Numerous studies in fMRI have shown that cannabis use can alter brain functioning, especially in networks that support working memory, attention and cognitive control processing.[13] More specifically, a recent systematic review found that a substantial number of studies (40%) conducted in cannabis users showed a higher positive resting state FC in fronto-frontal, fronto-temporal and fronto-striatal networks relative to controls.[14] Moreover, alterations of functional connectivity (FC) at rest have been reported in individuals with CUD relative to healthy controls, although their direction has shown mixed.[15] These contrasting findings are due in part to the temporal characteristics of FC. Indeed, FC cannot be considered stationary but varies over time with functional coupling between regions and networks that dynamically rearrange in various connectivity modes.[16] For this reason, the use of a static analysis approach may oversimplify a model that eventually fails to capture the complexity of brain FC.

Recently, to overcome these limitations, a new analytic framework, dFNC, that investigates the temporal changes of brain connectivity over time (and, for this reason, defined as 'chronnectome') has been developed.[16–21] DFNC studies the recurring patterns of FC between different functional brain networks, namely, FC 'states', that are reproducible over time and between different subjects.[17,22,23]

DFNC can be studied with two different and complementary methods: a cluster-state approach and a meta-state approach. The first is based on a deterministic assumption, with a subject dwelling in only a single state of connectivity at a given point in time, and reveals pairwise network connectivity patterns arranged in states and the changes in their temporal engagement.[16] The second arises from a probabilistic view of the connectivity states where a subject can occupy several states of connectivity at each time, 'meta-states',[24] and provides estimates of the overall dynamics of FC between states with metrics of dFNC fluidity and range.[16,24–27]

In this study, our major aim was to understand the role of altered dFNC in the development of CUD. For this, we wanted to identify alterations in dFNC in individuals at risk of CUD. Moreover, to confirm the possible role of these neural changes in the clinical presentation of CUD, we correlated dFNC measures with clinical variables in cannabis users. Notably, we recruited only individuals at risk of cannabis addiction: first, to understand the mechanisms associated with the development of the CUD and, second, to study the effects of cannabis use while reducing the confounding effects of clinical and psychosocial changes after the problematic use of cannabis.[28–31]

2 | MATERIALS AND METHODS

2.1 | Participants and MRI data

Ninety-eight subjects were initially recruited for this study. Exclusion criteria were considered: a present or past mental disorder assessed using the structured clinical interview (SCID) for the DSM-IV-TR; current or past substance use other than cannabis and nicotine; and history of neurological disorders, brain trauma or other concurrent drug treatment. None of the participants met the diagnostic criteria for the DSM-IV-TR cannabis use disorder. After recruitment, four participants were excluded for not having undergone an imaging session ($n = 3$) or clinical data appointment ($n = 1$). A final sample of 94 individuals (66 males and 28 females, aged between 18 and 30 years) was included in the study.

The following demographic data were collected: age, sex, handedness and education. All participants were also evaluated for depression, anxiety and ADHD using Hamilton Depression (HAM-D),[32,33] the State and Trait Anxiety Inventory (STAI-G X1, STAI-G X2)[34] and the German adult ADHD symptoms self-rated scale (Aufmerksamkeitsdefizit-/Hyperaktivitätsstörung im Erwachsenenalter, Selbstbeurteilungsskala, ADHS-SB).[35]

Participants were stratified according to their risk of developing CUD using a screening tool, the Cannabis Use Disorder Identification Test (CUDIT-R), with the risk of CUD defined by a score greater than or equal to 8 as reported previously,[36,37] thus resulting in 55 controls and 39 individuals at risk of CUD. Patterns of cannabis use (lifetime total cannabis use, age of onset, duration and current use [days/week and g/week]) were used to evaluate cannabis use (see Table 1).

Consumers were asked to abstain from cannabis use for at least 24 h before clinical assessment and MRI. Participants consented to these study-specific requirements, and no craving or other withdrawal symptoms were reported before the MRI scanning. The study was carried out in accordance with the Declaration of Helsinki, and the protocol was approved by the ethical review board of the Saarland Medical Association, Saarbrücken, Germany. Written informed consent was obtained from all participants after the study procedures had been fully explained.[38]

2.2 | MRI data acquisition

The scans were obtained using a 3T Magnetom-type Skyra (Siemens, Erlangen, Germany) MRI system. Images in structural MRI were acquired through rapid sequences prepared at gradient-echo magnetization (3D-MPRAGE) set with the following parameters: TE = 3.29 ms, TR = 1900 ms, TI = 110 ms, flip angle = 9°, FOV = 240 mm, slice plane = axial, voxel size = 0.5 × 0.5 × 0.9 mm^3, distance factor = 50%, number of slices = 192.

TABLE 1 Demographics, substance use characteristics and psychometric scores.

	Control s $n = 55$ Mean ± SD	CUD at-risk $n = 39$ Mean ± SD	p[a]
Age (years)	23.30 ± 3	23.20 ± 3.31	0.77
Sex (M:F)	30:25	36:3	0.006
Handedness (R:L)	52:3	36:3	0.202
Education (years)	14.90 ± 2.68	13.70 ± 2.57	0.033
HAM-D	0.364 ± 0.729	1.38 ± 2.22	0.002
STAI-G X1	31.00 ± 7.47	36.30 ± 8.03	0.001
STAI-G X2	31.50 ± 7.74	35.60 ± 8.75	0.018
ADHD-SB tot	6.110 ± 5.99	13.10 ± 6.94	<0.001
ADHS inattentive	2.98 ± 2.55	5.82 ± 3.10	<0.001
ADHS impulsivity	0.836 ± 1.13	2.18 ± 2.14	<0.001
ADHS hyperactivity	1.62 ± 2.21	3.03 ± 2.28	0.003
Tobacco per year (pack/year)	0.942 ± 3.090	2.50 ± 4.65	0.054
N. joints lifetime	2000 ± 8,430	3,258 ± 3,949	<0.001
CUDIT-R total	1.040 ± 2.04	16.90 ± 7.64	<0.001
Age of the first consume (years)	4.670 ± 8.17	17.70 ± 2.89	<0.001
Duration use (years)	0.373 ± 1.57	3.41 ± 3.39	<0.001
Current use (days/week)	0.473 ± 1.41	4.95 ± 2.32	<0.001
Current use (g/week)	0.212 ± 0.779	5.01 ± 5.53	<0.001

Note: Significant results are emboldened.
Abbreviations: ADHS-SB, ADHS-Selbstbeurteilungsskala; CUD, Cannabis use disorder; HAM-D, Hamilton Rating Scale for Depression; STAI-G X1, State–Trait Anxiety Inventory German version Form X1; STAI-G X2, State–Trait Anxiety Inventory German version Form X2.
[a]Results from two-sample t tests or Chi squared tests, when appropriate.

Then, rs-fMRI images were obtained using a BOLD echo-planar (EPI) sequence set with the following parameters: TE = 30 ms, TR = 1800 ms, flip angle = 90°, FOV = 192 mm, slice plane = transversal, voxel size = 3 × 3 × 3 mm, distance factor = 25%, number of slices = 32, PAT factor = 2, number of measurements = 230.

2.3 | MRI data analysis

After discarding the first eight scans, acquired to allow the signal to reach the steady state, 222 volumes were pre-processed.

Data Processing Assistant for rs-fMRI (DPABI/DPARSF 5.2) was used to pre-process the neuroimaging data.[39] A slice-timing correction was used to correct for temporal mismatch in slice acquisition. Next, realignment was used to correct head movements through rigid-body transformations and estimate motion extent. Functional and structural images were coregistered, segmented and normalized on a Montreal Neurological Institute (MNI) template using DARTEL.[40] Finally, a 6-mm 3D Gaussian kernel full width at half maximum was used for smoothing.

The data were decomposed into functional networks using a spatial group-independent component analysis (ICA),[41] implemented through the group ICA of fMRI toolbox (GIFT)[42] (https://trendscenter.org/software/gift/). The group information guided ICA (GIG-ICA) algorithm was used for constrained ICA on the NeuroMark template, which comprises 53 intrinsic connectivity networks (ICNs) that were estimated in two large independent samples and span across seven functional network domains: subcortical (SC), auditory (AUD), sensorimotor (SM), visual (VIS), cognitive-control (CC), default mode (DM) and cerebellar (CB).[43] To increase the reliability and stability of the estimation, the ICA was repeated 50 times using the ICASSO toolbox.[44,45]

2.4 | Dynamic functional network connectivity

DFNC was estimated using the GIFT toolbox, through sliding window analysis.[22,46] For each subject, the 53 (one for each ICN) time-courses (TC) were detrended, orthogonalized with respect to 12-motion parameters, despiked using 3dDespike (https://afni.nimh.nih.gov/pub/dist/doc/program_help/3dDespike.html) and, subsequently, filtered with a fifth-order Butterworth low-pass filter (cut-off of 0.15 Hz).[47] A sparse matrix of inverse covariance was calculated through a least absolute shrinkage and selection operator regression using an L1 penalty to improve the estimation of the shortest TC.[48] The matrix size resulted of 53 × 53 based on the number of ICNs. We used Gaussian windows with a size of 30 TR (54 s) and a sigma of 3 TR (5.4 s) to taper along the window edges advancing 1 TR at each step, resulting in 192 windows (see Figure 1). Then, the dFNC values were Fisher's Z-transformed and residualized with respect to significant nuisance covariates, including age, sex, education and motion (mean framewise displacement according to Power et al.[49]).

2.4.1 | Meta-state analysis

In the meta-state approach, dFNCs are modelled as the weighted sum of maximally statistically independent connectivity patterns. Each wFNC was decomposed into maximally independent prototype connectivity patterns (CPs) using a time-independent component analysis (tICA). CP's time courses underwent a transformation in the corresponding discretized quartile so that the weight of each pattern could be either positive or negative with respect to a space state, thus being in a pro-state or anti-state form if positive or negative, respectively. In this manner, a time-indexed vector of five dimensions was obtained, in which the time-course varied from one level to another. In this framework, a subject could be in more than one meta-state at a specific time point, and the probability of being in one meta-state changed dynamically.[24]

To calculate the individual connectivity patterns, the meta-state dFNC analysis was implemented through a temporal ICA (tICA), using the Infomax algorithm, with a model order of five, sufficient to include complex additive effects while maintaining a richly featured basis pattern according to the previous literature.[22,24] This analysis was repeated 10 times to obtain robust and reliable results using ICASSO.

To increase computational tractability, each value of a TC, derived from the regression of each subject dFNC information at each time window on the group of tICA connectivity patterns, was discretized into eight bins using its signed quartile, thus providing a pro-state (positive) and an anti-state (negative) score based on their sign, that corresponded to a specific meta-state.[24]

For each subject, four indices were estimated to summarize the dynamic properties of the networks and to describe the trajectory of the windowed correlations among different states (see Figure 1):

- Number of states: the overall number of distinct meta-states occupied.
- Change between states: the number of transitions from one meta-state to another.
- State span: the maximum L1 distance (distance in the cab geometry) between meta-states.
- Total distance: sum of L1 distances between successive meta-states, that is, the total distance travelled by each subject along state-space.[24]

2.4.2 | Cluster states analysis

The state-based dFNC analysis was implemented through a cluster state approach to identify dFNC states in the native state space. In this case, k-means clustering of wFNC matrices was repeated to reduce dimensionality. Each windowed functional connectivity matrix (wFNC) was defined by the value $N(N-1)/2$, where N represents the number of components of interest: K means clustering consists of a dimensional reduction technique that allows us to "collapse" the space connectivity of $N(N-1)/2 > 1{,}000$ dimensions into one, thus obtaining the most recurrent connectivity pattern: a subject will therefore be in a single specific state at any given moment.[22]

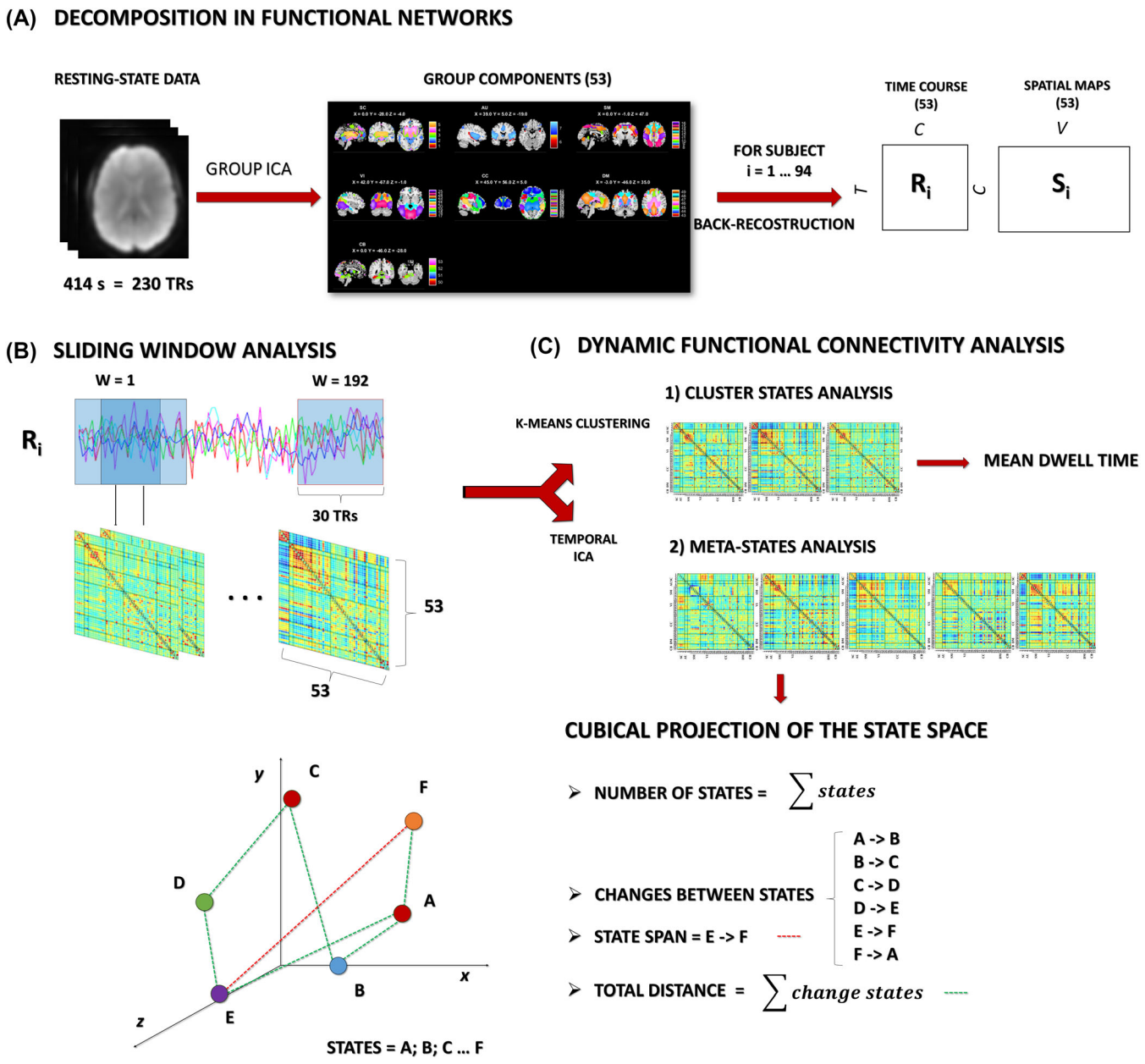

FIGURE 1 Graphical representation of the dFNC analysis process. (A) Resting-state data were decomposed using a spatial group ICA, thus identifying 53 group components according to the NeuroMark template, each composed of a time course (Ri) and a spatial map (Si). These components were then back-reconstructed at the subject level i. (B) A sliding window analysis was performed on the time courses. A window of 30 repetition times (TR) moved over the time course of 1 TR at a time, resulting in 192 windows. On each window a 53-by-53 functional connectivity matrix (wFNC) was calculated. (C) On the total of wFNCs: (1) a k-means clustering was used to identify the cluster states and the mean dwell time for each of them (the average time a subject stayed in the same state); (2) a temporal ICA was used to identify temporally independent components, the meta-states that spanned across a five-dimensional space and were described using several measures indicated on the bottom right of the figure. For display purposes, we displayed the metastate measures in a three-dimensional space (x, y, z). Each state is represented by a dot, and the path from one state to another is displayed using a dotted line. The number of states is calculated as the total of number of dots; the change between states is represented by the length of the green lines connecting two dots; the state span (red line) is the maximum distance between dots; the total distance is the sum of the length of each green line.

K-means clustering allowed us to identify the four most recurrent connectivity patterns, minimizing the total variance within the most similar matrices, and obtaining the states. The number of clusters or states was determined by the elbow criterion. For each FC cluster state, the mean dwell time, defined as the average time that each subject spent in a specific state, measured as the number of consecutive windows, was estimated[22] (see Figure 1). Cluster states that recurred in less than 10 individuals per sample were considered not reliable for group comparisons and excluded from further analysis.

2.5 | Statistical analysis

Statistical analyses were performed using JAMOVI[50] (https://www.jamovi.org/). Demographics, psychometric assessments, substance use patterns and brain dynamics indices were compared between samples using two-sample *t* tests. Brain dynamics indices were also correlated with clinical and substance use parameters using Pearson's correlations. Additionally, to take into account the psychopathological differences between samples, the analyses were repeated using analyses of covariance (ANCOVA) to compare group differences and partial correlations for brain-behaviour correlations with the score of each scale (HAM-D, STAI-G X1 and X2, and ADHS-SB) as nuisance covariates, respectively. Statistical significance was assessed using a threshold of $p = 0.05$, and a false discovery rate (FDR) correction with $\alpha = 0.05$ was used for multiple comparisons.[51]

TABLE 2 Comparison of the meta-state indexes between CUD at risk and controls.

	t	*p*[a]
Number of states	2.35	0.021
Change between states	2.43	0.017
State span	2.72	0.008
Total distance	3.36	0.001

[a]Results from two-sample *t* tests.

3 | RESULTS

3.1 | Meta-state analysis

The following brain dynamics indices were significantly increased in individuals at risk for CUD compared to controls (see Table 2 and Figure 2).

These results were confirmed by ANCOVAs with HAM-D, STAI-G X1, STAI-G X2 and ADHS-SB (see Table 3).

All correlation analyses carried out between meta-state measures and psychometric scores or consumption patterns were not significant.

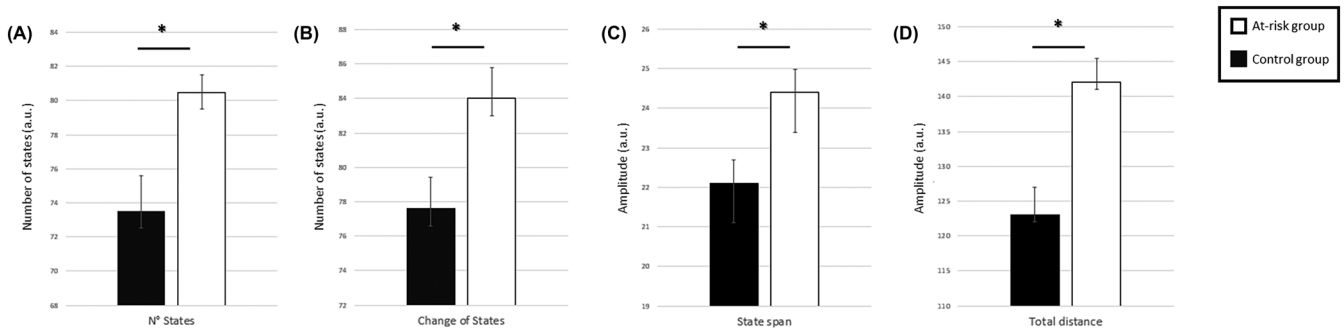

FIGURE 2 Brain dynamics estimated using meta-states is increased in individuals at risk for CUD. The bar plots represent the magnitude of the meta-states dynamic indices for each diagnostic group: (A) number of states, (B) changes of states, (C) state span and (D) total distance. A.U., arbitrary units. Error bars represent the standard error of the mean. *Significant difference between control and at risk subjects with a $p < 0.05$

TABLE 3 Comparisons of meta-state dynamic indices between CUD at risk and normal controls while taking into account each individual's psychopathology using ANCOVAs with HAM-D, STAI-G X1, STAI-G X2 and ADHS-SB scores as covariates.

HAM-D ANCOVA	***F***	***p***	**STAI-G X2 *ANCOVA***	***F***	***p***
Number of states	2.66	0.009	Number of states	2.09	0.039
Change between states	2.75	0.007	Change between states	2.21	0.030
State span	2.97	0.004	State span	2.41	0.018
Total distance	3.59	<0.001	Total distance	3.06	0.003
STAI-G X1 ANCOVA	***F***	***p***	**ADHS-SB ANCOVA**	***F***	***p***
Number of states	2.44	0.017	Number of states	1.74	0.086
Change between states	2.58	0.011	Change between states	1.77	0.080
State span	2.69	0.008	State span	2.52	0.013
Total distance	3.41	<0.001	Total distance	2.64	0.010

.

Abbreviations: ADHS-SB, ADHS-Selbstbeurteilungsskala; CUD, cannabis use disorder; HAM-D, Hamilton Rating Scale for Depression; STAI-G X1, State–Trait Anxiety Inventory German version Form X1; STAI-G X2, State–Trait Anxiety Inventory German version Form X2.

3.2 | Cluster state analysis

Four cluster states were estimated. After discarding state four data for limited reliability (see before), three clusters were further analysed (see Figure 3).

3.2.1 | Cluster State 1

State 1 recurred 15% of the time. In this state, the within-network correlations were highest in SC, SM and CC, and the between-network correlations were highest in SC (negative with SM and CC), SM (negative with VI and SC and positive with CC) and CC (negative with VI and SC and positive with SM).

3.2.2 | Cluster State 2

State 2 recurred 12% of the time. In this state, within-network correlations were highest in SC, SM and VI, and between-network correlations were highest in SM (negative with SC, DM, some CC ICs and positive with VI), SC (negative with SM, VI and CB and positive with DM), VI (negative with SC, positive with SM), DM (positive with SC and some CC ICS, negative with SM) and CB (negative with SC).

3.2.3 | Cluster State 3

State 3 recurred 29% of the time. In this state, within-network correlations were highest in SC, SM, VI, CC and DM, while between-network correlations were reduced for SC (with AU, SM and CC), AU (with SC, SM, VIS, CC and CB), SM (with SC, AU, VIS, CC and CB), VI (with SC, AU, SM and CB), for CC (with SC, AU, SM and CB) and CB (with AU, VIS and CC).

When comparing the dwell time between the groups, at-risk individuals dwelled longer only in State 3 relative to the control group ($t_{92} = 2.85$, $p = 0.005$) (see Figure 4). These results were confirmed by ANCOVAs with HAM-D ($t_{91} = 2.55$, $p = 0.013$), STAI-G X1 ($t_{91} = 2.54$, $p = 0.013$), STAI-G X2 ($t_{91} = 2.80$, $p = 0.006$) or ADHS-SB ($t_{91} = 2.31$, $p = 0.023$).

The mean dwell time in Cluster 3 and the psychometric scores or the cannabis use patterns were not significantly correlated.

4 | DISCUSSION

The aim of this study was the identification of dFNC alterations associated with the risk of CUD. This study yielded two main findings resulting by two complimentary approaches: at-risk individuals had a greater number of extremely volatile meta-states and moved more frequently between them, covering a greater distance in the state space, and, at the same time within specific cluster states, they tended to stay longer in a state (Cluster State 3) with high within-network coupling in SC, SM, VI, CC and DM, and reduced between-network coupling.

4.1 | Meta-state changes in the risk of CUD

The FC of the brain networks in the risk of CUD showed increased dynamics. In particular, a higher number of meta-states, and more frequent transitions from one meta-state to another, reflected greater dynamic fluidity in individuals at risk for CUD relative to those at low risk. Additionally, a greater maximal L1-distance between meta-states and the total distance travelled in the state space indicated a greater

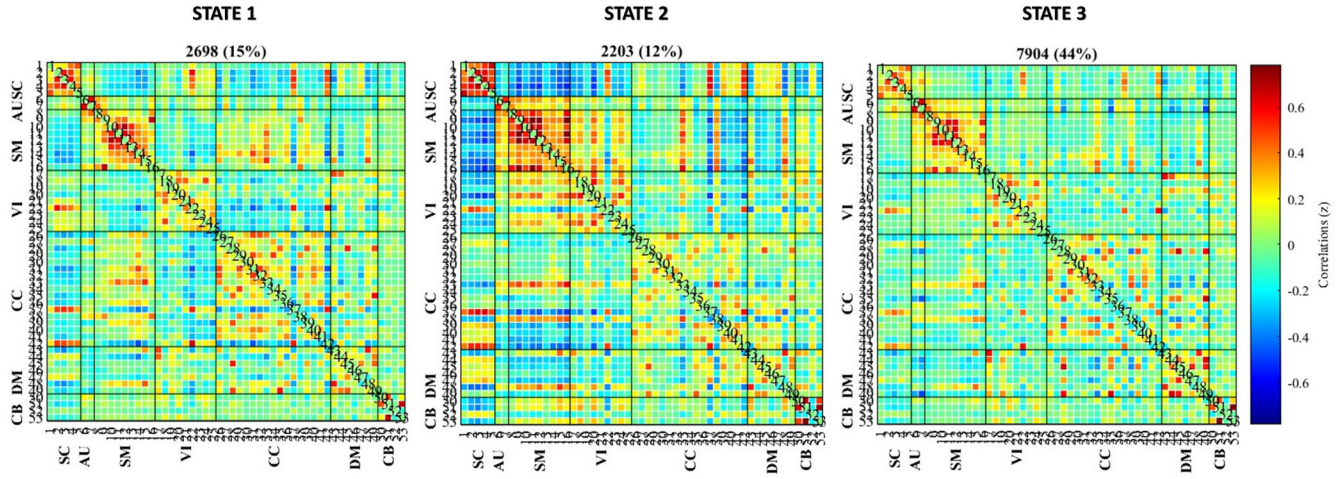

FIGURE 3 Cluster-state structure. For each cluster state, the centroid of 53 × 53 cross-correlation matrices was estimated using k-means clustering and ordered by functional network domain. Percentages indicate the number of windows where a cluster state was present relative to the total number of windows in the overall sample. The colour bar indicates the magnitude of each correlation. In SC, sub-cortical domain; AU, auditory domain; SM, sensorimotor domain; VI, visual domain; CC, cognitive-control domain; DM, default-mode domain; CB, cerebellar domain

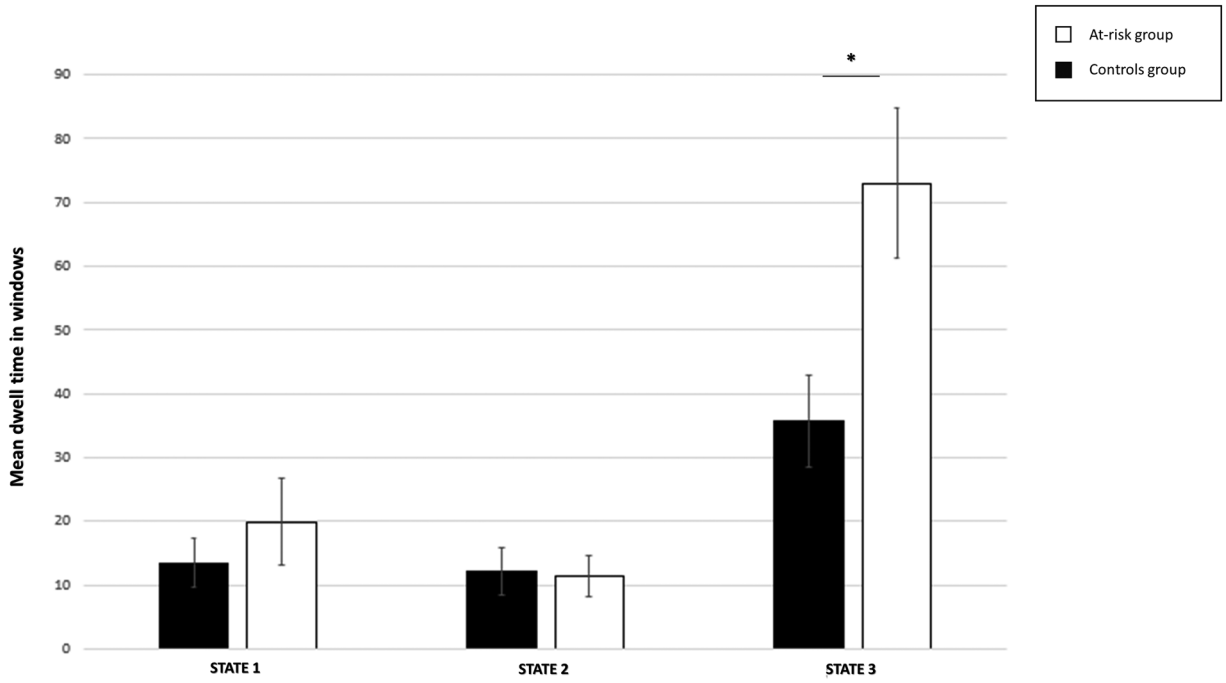

FIGURE 4 Individuals at risk for cannabis use disorder dwelled longer in State 3. The bar plot represents the mean dwell time of the three cluster states (see Figure 3 for the cluster structure). The dwell times are measured in units of repetition time (1 TR = 1.8 s). The error bars represent the standard error of the mean. *$p < 0.05$

dynamic range in at-risk individuals. Overall, at-risk individuals have more patterns of interrelationship between networks (meta-states) where they persist for shorter times, and temporally subsequent states differ more than in low-risk individuals.

Studies in neuropsychiatric disorders with cognitive impairments have shown conflicting results on dynamic functional connectivity, with some studies showing decreased values for all global brain dynamic indices in schizophrenia,[24] autism,[52] some forms of major neurocognitive disorder[26] and in preterm born adolescents,[53] and others showing higher values for these metrics, including Alzheimer's disease[54] and other neonatal disorders such as foetal alcohol spectrum disorder.[55]

Consistent with these studies, we found a subtle cognitive impairment indicated by inattention, hyperactivity and impulsivity scales in subjects at risk for CUD. To reconcile these findings, we can hypothesize that dynamic features could be related to the subject global cognitive functioning following an inverted-U model, so that subjects with low or high dynamic indices have impaired cognition, in the first case due to the lower possibility of configuring adaptive networks, while in the second, this is due to an instability in maintaining efficient and goal-oriented networks with frequent changes between distant states.

4.2 | Cluster state features in the risk of CUD

These individuals persist longer in a state characterized by higher intra-network connectivity in the subcortical, sensorimotor, visual, default mode and cognitive-control network domains and reduced between-network interactions. The subcortical network domain includes the nucleus accumbens, the ventral tegmental area (VTA), the basolateral amygdala, the hippocampus, the bed nucleus of the stria terminalis, the dorsolateral striatum and the globus pallidus. THC activates presynaptic CB1 receptors (CB1R) in VTA GABAergic neurons that inhibit presynaptic GABA release, and this causes increased dopaminergic firing in the VTA, which may explain the greater intrinsic activity of this network.[56] The subcortical regions are connected to the prefrontal regions through dopaminergic and GABAergic projections. The cognitive control network, including the prefrontal regions, plays a role in cognition, emotional regulation, salience and impulsivity that can be altered in cannabis use and dependence.[57] Therefore, connectivity between subcortical and cognitive control networks can be crucial for the recognition of a reward in the environment and in complex affective and cognitive behaviours, including the formation and retrieval of associative and contextual fear- and reward-related memories.[57] Altered functional connectivity of the subcortical network domain has been reported in previous studies,[14] thus suggesting that changes in dynamic connectivity may be related to altered reward processing and disinhibition. Altered dynamic connectivity of sensorimotor and visual networks supports a modulatory role of cannabis use on sensorimotor function. In this regard, it is noteworthy that recent studies have shown that individuals with high THC use have more severe neurological soft signs (NSS) compared to controls.[58] This is probably caused by an impairment of the sensorimotor system through direct stimulation of CB1R and an alteration of dopamine signalling in the limbic/associative and sensorimotor cortical regions due to THC.[58] Furthermore, the activity of the visual network appears to

be influenced by cannabis use and is related to the development of NSS. A recent study demonstrated that chronic cannabis consumers have greater activation during a visual attention task not only in the occipital cortex but also in various frontal and parietal regions, suggesting compensatory and adaptive processes to maintain physiological network functioning.[59] Even the default mode network, particularly in the posterior regions, has been implicated in THC dependence.[60] Hyperactivation of this network is related to greater sensitization to drug-seeking behaviours and decreased performance on strategic decision-making tests,[61,62] which supports the role of these changes in the development of addiction.

Overall, our findings are in accordance with the GABA-glutamatergic hypothesis of CUD, which posits that THC can modulate the neuronal excitability of the brain circuits by regulating GABA and glutamate signalling.[60,63] CB1Rs, which are more expressed at the level of GABAergic neurons, are activated by endocannabinoids and inhibit neurotransmitter release through retrograde synaptic transmission. GABAergic interneurons, especially fast-spiking parvalbumin (PV)-expressing interneurons and non-fast spiking cholecystokinin (CCK)-positive cells, play a substantial role in the synchronization of large numbers of glutamatergic pyramid cells. CCK-positive cells that express CB1R work as a noise filter to remove high-frequency signals from pyramidal cells. Endocannabinoids can determine a fine-tuning of cortical neural oscillations by modulating these interneurons. Therefore, the disruption of endocannabinoid signalling caused by CB1R downregulation in chronic cannabis users appears to disrupt excitatory-inhibitory balance and affects dynamic connectivity, causing a major disruption in network interaction with cortical and subcortical domains that function more independently of each other.[64]

4.3 | Strengths and limitations

This study has some potential limitations. First, the relatively small sample size reduces the potential of detecting more subtle associations and therefore the representativeness of our findings. However, our design was sufficiently powerful to detect the moderate-higher differences with a robust correction for multiple comparisons to avoid Type II errors. Future studies with larger sample sizes are warranted for the replication of these results.

Second, anxiety and ADHD scores were higher in at-risk subjects relative, and this could have partially contributed to our findings. Notably, most subjects had scores below the clinical cut-off, thus suggesting a limited impact of these variables, if any, that could be efficiently accounted for using these scores as nuisance covariates. Finally, our cross-sectional study does not allow for the evaluation of trajectory risk.

5 | CONCLUSION

This is the first study to evaluate dynamic connectivity in individuals at risk for CUD. We have shown that individuals at risk for CUD present, early in the course of cannabis use, a global alteration of the dynamics of brain network interplay with specific changes in subcortical and cortical circuits.

DFNC alterations can contribute to the identification of prognostic factors in individuals at risk of CUD, in whom preventive intervention can be carried out, and of novel targets for treatment. DFNC alterations could also be used as biomarkers in preclinical pharmacological trials to test drug efficacy to normalize the dFNC of at-risk individuals' disruption to avoid their progression to addiction. Finally, longitudinal studies are needed to establish the relationship between functional connectivity dynamics and the development of cannabis use disorder to confirm their role as biomarkers of the risk.

AUTHOR CONTRIBUTIONS

Fabio Sambataro, Robert Christian Wolf, Miriam Wittemann, Nadine D. Wolf, Wolfgang Reith, Florian Werler, Katharina M. Kubera, Vince D Calhoun and Dusan Hirjak were responsible for the study concept and design. Robert Christian Wolf, Florian Werler, Miriam Wittemann and Wolfgang Reith contributed to the acquisition of clinical and neuroimaging data. Giovanni Fazio, Daniele Olivo and Fabio Sambataro performed neuroimaging and statistical analyses and assisted with data analysis and interpretation of the findings. Giovanni Fazio and Fabio Sambataro drafted the first version of the manuscript. Robert Christian Wolf, Dusan Hirjak and Mike M. Schmitgen provided critical revision of the manuscript for important intellectual content. All authors critically reviewed the content and approved the final version for publication.

ACKNOWLEDGEMENTS

We thank all study participants for their understanding and willingness to participate in this study.

CONFLICT OF INTEREST STATEMENT

The authors declare that no competing financial interest exists.

DATA AVAILABILITY STATEMENT

The data that support the findings of this study are available from the corresponding author upon reasonable request.

ETHICS STATEMENT

The study was carried out in accordance with the Code of Ethics of the World Medical Association (Declaration of Helsinki) for experiments involving humans. All participants gave their informed written consent as approved by the Ethics Review Board of the Saarland Medical Association, Saarbrücken, Germany.

ORCID

Dusan Hirjak https://orcid.org/0000-0003-1226-9800
Mike M. Schmitgen https://orcid.org/0000-0002-6475-7155
Robert Christian Wolf https://orcid.org/0000-0002-5358-5212
Fabio Sambataro https://orcid.org/0000-0003-2102-416X

REFERENCES

1. UN drug report shines light on cannabis, cocaine and methamphetamine trends|UN News. https://news.un.org/en/story/2022/06/1121472 (accessed 2023-02-12).
2. World Health Organization. *Health and Social Effects of Nonmedical Cannabis Use (The)*. World Health Organization; 2016.
3. Hallam C, Bewley-Taylor DR. Mapping the world drug problem: science and politics in the United Nations drug control system. *Int. J. Drug Policy*. 2010;21(1):1-3. doi:10.1016/j.drugpo.2009.10.007
4. Patel J, Marwaha R. Cannabis Use Disorder. In: *StatPearls*. StatPearls Publishing; 2022.
5. Carney R, Cotter J, Firth J, Bradshaw T, Yung AR. Cannabis use and symptom severity in individuals at ultra high risk for psychosis: a meta-analysis. *Acta Psychiatr. Scand.* 2017;136(1):5-15. doi:10.1111/acps.12699
6. Sideli L, Quigley H, La Cascia C, Murray RM. Cannabis use and the risk for psychosis and affective disorders. *J. Dual Diagn.* 2020;16(1):22-42. doi:10.1080/15504263.2019.1674991
7. Urits I, Gress K, Charipova K, et al. Cannabis use and its association with psychological disorders. *Psychopharmacol. Bull.* 2020;50(2):56-67.
8. Association of smoked cannabis with treatment resistance in schizophrenia - PubMed. https://pubmed.ncbi.nlm.nih.gov/31229838/ (accessed 2023-03-16).
9. Cannabis use: epidemiology, pharmacology, comorbidities, and adverse effects - UpToDate. https://www.uptodate.com/contents/cannabis-use-epidemiology-pharmacology-comorbidities-and-adverse-effects?topicRef=7796&source=see_link (accessed 2023-03-16).
10. Koob GF, Volkow ND. Neurocircuitry of addiction. *Neuropsychopharmacology*. 2010;35(1):217-238. doi:10.1038/npp.2009.110
11. Zehra A, Burns J, Liu CK, et al. Cannabis addiction and the brain: a review. *J. Neuroimmune Pharmacol.* 2018;13(4):438-452. doi:10.1007/s11481-018-9782-9
12. Lee MH, Smyser CD, Shimony JS. Resting-state fMRI: a review of methods and clinical applications. *AJNR Am. J. Neuroradiol.* 2013;34(10):1866-1872. doi:10.3174/ajnr.A3263
13. Burggren AC, Shirazi A, Ginder N, London ED. Cannabis effects on brain structure, function, and cognition: considerations for medical uses of cannabis and its derivatives. *Am. J. Drug Alcohol Abuse*. 2019;45(6):563-579. doi:10.1080/00952990.2019.1634086
14. Thomson H, Labuschagne I, Greenwood L-M, et al. Is resting-state functional connectivity altered in regular cannabis users? A systematic review of the literature. *Psychopharmacology (Berl)*. 2022;239(5):1191-1209. doi:10.1007/s00213-021-05938-0
15. Lichenstein SD, Manco N, Cope LM, et al. Systematic review of structural and functional neuroimaging studies of cannabis use in adolescence and emerging adulthood: evidence from 90 studies and 9441 participants. *Neuropsychopharmacology*. 2022;47(5):1000-1028. doi:10.1038/s41386-021-01226-9
16. Calhoun VD, Miller R, Pearlson G, Adalı T. The chronnectome: time-varying connectivity networks as the next frontier in fMRI data discovery. *Neuron*. 2014;84(2):262-274. doi:10.1016/j.neuron.2014.10.015
17. Chang C, Glover GH. Time-frequency dynamics of resting-state brain connectivity measured with fMRI. *Neuroimage*. 2010;50(1):81-98. doi:10.1016/j.neuroimage.2009.12.011
18. Canolty RT, Ganguly K, Kennerley SW, et al. Oscillatory phase coupling coordinates anatomically dispersed functional cell assemblies. *Proc. Natl. Acad. Sci. U. S. A.* 2010;107(40):17356-17361. doi:10.1073/pnas.1008306107
19. Fries P. A mechanism for cognitive dynamics: neuronal communication through neuronal coherence. *Trends Cogn. Sci.* 2005;9(10):474-480. doi:10.1016/j.tics.2005.08.011
20. Hillebrand A, Tewarie P, van Dellen E, et al. Direction of information flow in large-scale resting-state networks is frequency-dependent. *Proc. Natl. Acad. Sci. U. S. A.* 2016;113(14):3867-3872. doi:10.1073/pnas.1515657113
21. Sakoğlu U, Pearlson GD, Kiehl KA, Wang YM, Michael AM, Calhoun VD. A method for evaluating dynamic functional network connectivity and task-modulation: application to schizophrenia. *MAGMA*. 2010;23(5–6):351-366. doi:10.1007/s10334-010-0197-8
22. Allen EA, Damaraju E, Plis SM, Erhardt EB, Eichele T, Calhoun VD. Tracking whole-brain connectivity dynamics in the resting state. *Cereb. Cortex*. 2014;24(3):663-676. doi:10.1093/cercor/bhs352
23. Marusak HA, Calhoun VD, Brown S, et al. Dynamic functional connectivity of neurocognitive networks in children. *Hum. Brain Mapp.* 2017;38(1):97-108. doi:10.1002/hbm.23346
24. Miller RL, Yaesoubi M, Turner JA, et al. Higher dimensional meta-state analysis reveals reduced resting fMRI connectivity dynamism in schizophrenia patients. *PLoS ONE*. 2016;11(3):e0149849. doi:10.1371/journal.pone.0149849
25. Preti MG, Bolton TA, Van De Ville D. The dynamic functional connectome: state-of-the-art and perspectives. *Neuroimage*. 2017;160:41-54. doi:10.1016/j.neuroimage.2016.12.061
26. Premi E, Calhoun VD, Diano M, et al. The inner fluctuations of the brain in presymptomatic frontotemporal dementia: the chronnectome fingerprint. *Neuroimage*. 2019;189:645-654. doi:10.1016/j.neuroimage.2019.01.080
27. Liu J, Liao X, Xia M, He Y. Chronnectome fingerprinting: identifying individuals and predicting higher cognitive functions using dynamic brain connectivity patterns. *Hum. Brain Mapp.* 2018;39(2):902-915. doi:10.1002/hbm.23890
28. Degenhardt L, Hall W, Lynskey M. Exploring the association between cannabis use and depression. *Addiction*. 2003;98(11):1493-1504. doi:10.1046/j.1360-0443.2003.00437.x
29. Kedzior KK, Laeber LT. A positive association between anxiety disorders and cannabis use or cannabis use disorders in the general population- a meta-analysis of 31 studies. *BMC Psychiatry*. 2014;14(1):136. doi:10.1186/1471-244X-14-136
30. Strohbeck-Kuehner P, Skopp G, Mattern, R. Cannabis improves symptoms of ADHD.
31. Volkow ND, Swanson JM, Evins AE, et al. Effects of cannabis use on human behavior, including cognition, motivation, and psychosis: a review. *JAMA Psychiatry*. 2016;73(3):292-297. doi:10.1001/jamapsychiatry.2015.3278
32. Jackson-Koku G. Beck depression inventory. *Occup. Med.* 2016;66(2):174-175. doi:10.1093/occmed/kqv087
33. Hamilton M. A rating scale for depression. *J. Neurol. Neurosurg. Psychiatry*. 1960;23(1):56-62. doi:10.1136/jnnp.23.1.56
34. Endler NS, Kocovski NL. State and trait anxiety revisited. *J. Anxiety Disord.* 2001;15(3):231-245. doi:10.1016/S0887-6185(01)00060-3
35. Rösler M, Retz W, Retz-Junginger P, et al. Instrumente zur diagnostik der aufmerksamkeitsdefizit-/hyperaktivitätsstörung (ADHS) im erwachsenenalter. *Nervenarzt*. 2004;75(9):888-895. doi:10.1007/s00115-003-1622-2
36. Adamson SJ, Sellman JD. A prototype screening instrument for cannabis use disorder: the cannabis use disorders identification test (CUDIT) in an alcohol-dependent clinical sample. *Drug Alcohol Rev.* 2003;22(3):309-315. doi:10.1080/0959523031000154454
37. Adamson SJ, Kay-Lambkin FJ, Baker AL, et al. An improved brief measure of cannabis misuse: the cannabis use disorders identification test-revised (CUDIT-R). *Drug Alcohol Depend.* 2010;110(1):137-143. doi:10.1016/j.drugalcdep.2010.02.017
38. Wolf RC, Werler F, Wittemann M, et al. Structural correlates of sensorimotor dysfunction in heavy cannabis users. *Addict. Biol.* 2021;26(5):e13032. doi:10.1111/adb.13032

39. Yan C, Zang Y. DPARSF: a MATLAB toolbox for "pipeline" data analysis of resting-state fMRI. *Front. Syst. Neurosci.* 2010;4:13. doi:10.3389/fnsys.2010.00013
40. Ashburner J. A fast diffeomorphic image registration algorithm. *Neuroimage*. 2007;38(1):95-113. doi:10.1016/j.neuroimage.2007.07.007
41. Wang C, Ong JL, Patanaik A, Zhou J, Chee MWL. Spontaneous eyelid closures link vigilance fluctuation with fMRI dynamic connectivity states. *Proc. Natl. Acad. Sci. U. S. A.* 2016;113(34):9653-9658. doi:10.1073/pnas.1523980113
42. Calhoun VD, Adali T, Pearlson GD, Pekar JJ. A method for making group inferences from functional MRI data using independent component analysis. *Hum. Brain Mapp.* 2001;14(3):140-151. doi:10.1002/hbm.1048
43. Du Y, Fu Z, Sui J, et al. NeuroMark: an automated and adaptive ICA based pipeline to identify reproducible fMRI markers of brain disorders. *NeuroImage Clin.* 2020;28:102375. doi:10.1016/j.nicl.2020.102375
44. Wei P, Bao R, Fan Y. Comparing the reliability of different ICA algorithms for fMRI analysis. *PLoS ONE*. 2022;17(6):e0270556. doi:10.1371/journal.pone.0270556
45. Bell AJ, Sejnowski TJ. An information-maximization approach to blind separation and blind deconvolution. *Neural Comput.* 1995;7(6):1129-1159. doi:10.1162/neco.1995.7.6.1129
46. Damaraju E, Allen EA, Belger A, et al. Dynamic functional connectivity analysis reveals transient states of dysconnectivity in schizophrenia. *NeuroImage: Clin.* 2014;5:298-308. doi:10.1016/j.nicl.2014.07.003
47. Abrol A, Chaze C, Damaraju E, Calhoun VD. The chronnectome: evaluating replicability of dynamic connectivity patterns in 7500 resting fMRI datasets. *Annu. Int. Conf. IEEE Eng. Med. Biol. Soc.* 2016;2016:5571-5574. doi:10.1109/EMBC.2016.7591989
48. Ranstam J, Cook JA. LASSO regression. *Br. J. Surg.* 2018;105(10):1348. doi:10.1002/bjs.10895
49. Power JD, Barnes KA, Snyder AZ, Schlaggar BL, Petersen SE. Spurious but systematic correlations in functional connectivity MRI networks arise from subject motion. *Neuroimage*. 2012;59(3):2142-2154. doi:10.1016/j.neuroimage.2011.10.018
50. Navarro DJ, Foxcroft DR. *Learning statistics with Jamovi: a tutorial for psychology students and other beginners*; 2018. doi:10.24384/HGC3-7P15
51. Benjamini Y, Hochberg Y. Controlling the false discovery rate: a practical and powerful approach to multiple testing. *J. R. Stat. Soc. B. Methodol.* 1995;57(1):289-300. doi:10.1111/j.2517-6161.1995.tb02031.x
52. Fu Z, Tu Y, Di X, et al. Transient increased thalamic-sensory connectivity and decreased whole-brain dynamism in autism. *Neuroimage*. 2019;190:191-204. doi:10.1016/j.neuroimage.2018.06.003
53. Lahti K, Setänen S, Vorobyev V, Nyman A, Haataja L, Parkkola R. Altered temporal connectivity and reduced meta-state dynamism in adolescents born very preterm. *Brain Commun.* 2023;5(1):fcad009. doi:10.1093/braincomms/fcad009
54. Ghanbari M, Zhou Z, Hsu L-M, et al. Altered connectedness of the brain chronnectome during the progression to Alzheimer's disease. *Neuroinformatics*. 2022;20(2):391-403. doi:10.1007/s12021-021-09554-3
55. Candelaria-Cook FT, Schendel ME, Flynn L, Cerros C, Hill DE, Stephen JM. Disrupted dynamic functional network connectivity in fetal alcohol spectrum disorders. *Alcohol. Clin. Exp. Res.* 2023;47(4):687-703. doi:10.1111/acer.15046
56. Lupica CR, Riegel AC. Endocannabinoid release from midbrain dopamine neurons: a potential substrate for cannabinoid receptor antagonist treatment of addiction. *Neuropharmacology*. 2005;48(8):1105-1116. doi:10.1016/j.neuropharm.2005.03.016
57. Curran HV, Freeman TP, Mokrysz C, Lewis DA, Morgan CJA, Parsons LH. Keep off the grass? Cannabis, cognition and addiction. *Nat. Rev. Neurosci.* 2016;17(5):293-306. doi:10.1038/nrn.2016.28
58. Wolf RC, Werler F, Schmitgen MM, et al. Functional correlates of neurological soft signs in heavy cannabis users. *Addict. Biol.* 2023;28(3):e13270. doi:10.1111/adb.13270
59. Chang L, Yakupov R, Cloak C, Ernst T. Marijuana use is associated with a reorganized visual-attention network and cerebellar Hypoactivation. *Brain*. 2006;129(Pt 5):1096-1112. doi:10.1093/brain/awl064
60. Katona I, Sperlágh B, Sík A, et al. Presynaptically located CB1 cannabinoid receptors regulate GABA release from axon terminals of specific hippocampal interneurons. *J. Neurosci.* 1999;19(11):4544-4558. doi:10.1523/JNEUROSCI.19-11-04544.1999
61. Filbey FM, Dunlop J, Ketcherside A, et al. fMRI study of neural sensitization to hedonic stimuli in long-term, daily cannabis users. *Hum. Brain Mapp.* 2016;37(10):3431-3443. doi:10.1002/hbm.23250
62. Prashad S, Dedrick ES, To WT, Vanneste S, Filbey FM. Testing the role of the posterior cingulate cortex in processing salient stimuli in cannabis users: an rTMS study. *Eur. J. Neurosci.* 2019;50(3):2357-2369. doi:10.1111/ejn.14194
63. Herkenham M, Lynn AB, Little MD, et al. Cannabinoid receptor localization in brain. *Proc. Natl. Acad. Sci. U. S. A.* 1990;87(5):1932-1936. doi:10.1073/pnas.87.5.1932
64. Syed SA, Schnakenberg Martin AM, Cortes-Briones JA, Skosnik PD. The relationship between cannabinoids and neural oscillations: how cannabis disrupts sensation, perception, and cognition. *Clin. EEG Neurosci.* 2022;54(4):359-369. doi:10.1177/15500594221138280

How to cite this article: Fazio G, Olivo D, Wolf ND, et al. The risk of cannabis use disorder is mediated by altered brain connectivity: A chronnectome study. *Addiction Biology*. 2024;29(5):29(5):e13395. doi:10.1111/adb.13395